Transcriptional Profiling of Macrophages Reveals Distinct Parasite Stage-driven Signatures During Early Infection by Leishmania Donovani

Visnu Chaparro
Institut National de la Recherche Scientifique (INRS) – Centre Armand-Frappier Santé Biotechnologie (AFSB)

Tyson E. Graber
Children's Hospital of Eastern Ontario Research Institute

Tommy Alain
Department of Biochemistry, Microbiology and Immunology, University of Ottawa

Maritza Jaramillo (maritza.jaramillo@inrs.ca)
Institut National de la Recherche Scientifique (INRS) – Centre Armand-Frappier Santé Biotechnologie (AFSB)

Research Article

Keywords: mRNA abundance, Leishmania donovani, promastigote, amastigote, macrophage, RNAseq

Posted Date: October 8th, 2021

DOI: https://doi.org/10.21203/rs.3.rs-944153/v1

Version of Record: A version of this preprint was published at Scientific Reports on April 16th, 2022. See the published version at https://doi.org/10.1038/s41598-022-10317-6.

Transcriptional profiling of macrophages reveals distinct parasite stage-driven signatures during early infection by *Leishmania donovani*

Visnu Chaparro[a], Tyson E. Graber[b], Tommy Alain[b,c], Maritza Jaramillo[a,1]

[a]Institut National de la Recherche Scientifique (INRS) – Centre Armand-Frappier Santé Biotechnologie (AFSB), Laval, Quebec, Canada

[b]Children's Hospital of Eastern Ontario Research Institute, Ottawa, Ontario, Canada

[c]Department of Biochemistry, Microbiology and Immunology, University of Ottawa, Ottawa, Ontario, Canada

[1]Correspondence should be addressed to: maritza.jaramillo@inrs.ca

INRS – CAFSB, 531 boul. des Prairies, Laval, Québec, H7V 1B7, Canada

Tel.: +1 (450) 687-5010 ext. 8872; fax: +1 (450) 686-5566

Keywords: mRNA abundance, *Leishmania donovani*, promastigote, amastigote, macrophage, RNAseq

Abstract

Macrophages undergo swift changes in mRNA abundance upon pathogen invasion. Herein we describe early remodelling of the macrophage transcriptome during infection by amastigotes or promastigotes of *Leishmania donovani*. Approximately 10% - 16% of host mRNAs were differentially modulated in *L. donovani*-infected macrophages when compared to uninfected controls. This response was partially stage-specific as a third of changes in mRNA abundance were either exclusively driven by one of the parasite forms or significantly different between them. Gene ontology analyses identified categories associated with immune functions (e.g. antigen presentation and leukocyte activation) among significantly downregulated mRNAs while cytoprotective-related categories (e.g. DNA repair and apoptosis inhibition) were enriched in upregulated transcripts during amastigote infection. Interestingly a combination of upregulated (e.g. cellular response to IFNβ) and repressed (e.g. leukocyte activation, chemotaxis) immune-related transcripts were overrepresented in the promastigote-infected dataset. In addition, Ingenuity Pathway Analysis (IPA®) coupled specific mRNA subsets with a number of upstream transcriptional regulators predicted to be modulated in macrophages infected with *L. donovani* amastigotes (e.g. STAT1 inhibition) or promastigotes (e.g. NRF2, IRF3, and IRF7 activation). Overall, our results indicate that early parasite stage-driven transcriptional remodelling in macrophages contributes to orchestrate both protective and deleterious host cell responses during *L. donovani* infection.

Introduction

Macrophages are the main replicative niche of protozoan parasites of the genus *Leishmania*, the etiologic agents of a spectrum of vector-borne diseases known as leishmaniases[1]. Within macrophages, sandfly-transmitted *Leishmania* promastigotes transform into amastigotes while subverting numerous host cell processes and immunological functions to ensure its proliferation[1]. Visceral leishmaniasis (VL) is a life-threatening disease that is caused by *L. donovani* and *L. infantum* (syn. *L. chagasi*)[2]. VL is endemic in more than 60 countries where it represents a severe public health concern due to the lack of vaccines and the emergence of parasite drug resistance[3]. Hence, a better understanding of the molecular events occurring at the host cell–parasite interface is critical to target novel regulatory nodes for therapeutic intervention.

Early remodelling of the transcriptome has been reported in macrophages during bacterial and parasitic infections[4-7]. Even though *Leishmania* promastigotes elicit the activation of anti-parasitic intracellular signals in macrophages as early as 15 min post-infection (p.i.) (e.g. MAPK p38 phosphorylation)[8], they are able to dampen host cell responses involved in pathogen clearance within 2 - 6 h.p.i. (e.g. phagolysosome maturation, antigen presentation, oxidative burst, and apoptosis)[1,9-11]. Consistent with this, rapid modulation of multiple transcription factors (e.g. STAT1, NRF2, IRF3 and IRF7) has been associated with either parasite persistence or host cell defense mechanisms against *L. donovani*[12-15]. Surprisingly, global-scale transcriptional profiling of *L. donovani*-infected macrophages has only been documented at ≥ 12 h.p.i.[16-20]. Therefore, currently available datasets may not reflect the totality of changes in gene expression programs that trigger, or are elicited by, early macrophage responses during *L. donovani* infection. Of note, to the best of our knowledge, no high throughput study comparing early transcriptional changes in

64 macrophages driven by both stages of *L. donovani* is available to date. Herein, using *L. donovani*
65 amastigote- and promastigote-infected RNA sequencing (RNAseq) datasets, we describe broad
66 and selective changes in the transcriptome of *L. donovani*-infected macrophages that are likely to
67 tailor key cellular responses involved in host defense but also in disease progression during VL.
68

Results

Infection with *L. donovani* amastigotes or promastigotes promotes early changes in the mRNA pool of the host cell

To compare the early effects of the two life stages *L. donovani* in the mature mRNA pool of the host cell, total cytosolic mRNA extracts from bone marrow-derived macrophage (BMDM) cultures infected with amastigote (AMA) or promastigote (PRO) parasites for 6 h were subjected to RNAseq and compared to non-infected controls (CTR) (**Fig 1A**). As shown by a projection of a principal component analysis, infection appears to be the main source of variation (37.4%) between the different datasets followed by a distinctive profile of the AMA-infected samples (**Fig 1B**). Differentially regulated mRNAs were identified using the *anota2seq* algorithm with a false discovery rate (FDR) ≤ 0.05 and a $\log_2$ expression fold-change ≥ 1.0. Out of 9442 mRNAs detected in BMDMs, 9.9% showed differential abundance during *L. donovani* amastigote infection (65.6% upregulated and 34.4% downregulated) (**Fig 1C** left panel and **Table S1**) while 15.8% were altered in BMDMs following infection with the promastigote stage (54.4% upregulated and 45.6% downregulated) (**Fig 1C** right panel and **Table S1**). These data indicate that infection by either amastigotes or promastigotes of *L. donovani* leads to early reprograming of the mRNA content of the host cell.

L. donovani amastigote infection modulates the abundance of mRNAs linked to different macrophage cellular processes

Gene Ontology (GO) hierarchical clustering analysis was carried out to determine whether subsets of mRNAs encoding functionally related proteins are selectively modulated in BMDMs upon infection with *L. donovani* amastigotes (**Fig 2A** and **Table S2**). Enrichment of functional

92 categories related to regulation of gene expression, positive regulation of DNA repair, and negative
93 regulation of apoptosis and protein modification was detected in the AMA-upregulated dataset
94 (**Fig 2A** upper panel, and **Table S2**). Targets in these categories included transcripts that encode
95 transcription (*Bdp1*, *Gtf3c6*, *Polr3f*, *Polr3g*), splicing (*Hnrnpa3*, *Hnrnpu*, *Sf3a2*, *Srsf1*) and
96 translation (*Dhx29*, *Eif1a*, *Eif3a*, *Eif4g2*) factors, proteins involved in DNA repair (*Lig4*, *Mdc1*,
97 *Smc6*, *Topbp1*), and inhibitors of apoptosis (*Bcl2*, *Hdac2*, *Hsph1*, *Mdm2*) (**Fig 2B**). In contrast,
98 categories associated with immune response, cell adhesion, signal transduction, protein refolding,
99 and cell cycle were enriched in the AMA-downregulated dataset (**Fig 2A** bottom panel and **Table**
100 **S2**). Accordingly, lower levels of transcripts encoding innate and adaptive immune mediators
101 (*Aif1*, *C1rb*, *Ccl5*, *Ifitm3*, *Il18bp*, *Irf7*, *Ly86*, *Lyz1*, *Nfil3*, *Ptger3*, *Tnfrsf14*), regulators of antigen
102 presentation (*Cd74*, *H2-Aa*, *H2-Ab1*, *H2-Eb1*, *Unc93b1*), and adhesion molecules (*Icam1*, *Itgal*,
103 *Itgb7*, *Rac2*) were detected in BMDMs infected with *L. donovani* amastigotes (**Fig 2B**).
104
105 **Functional groups of transcripts are modulated in macrophages upon *L. donovani***
106 **promastigote infection**
107 Enriched GO categories in upregulated transcripts of *L. donovani* promastigote-infected
108 macrophages revealed contrasting groups of activating (i.e. *Cxcl10*, *Cxcl3*, *Gbp3*, *Ifit1*, *Ifit2*,
109 *Irgm1*, *Tnf*) and inhibitory immune factors (*Cd200*, *Cd24a*, *Cd274*, *Cebpb*, *Nlrc5*, *Serpinb9*, *Socs1*)
110 (**Fig 3A** upper panel, **Fig 3B** and **Table S2**). In parallel, mRNAs encoding proteins associated with
111 cell survival (*Hmox1*, *Hsp90ab1*, *Optn*, *Wfs1*), iron transport (*Slc11a2*, *Slc25a37*, *Slc39a14*,
112 *Slc40a1*) and redox homeostasis (*Cat*, *Gclm*, *Gsr*, *Prdx1*, *Sod2*, *Txnrd1*) were also overrepresented
113 in the upregulated dataset (**Fig 3A** upper panel, **Fig 3B** and **Table S2**). In contrast, GO categories
114 related to cell death (*Casp2*, *Casp6*, *Cradd*, *Dfna5*, *Dusp6*, *Mef2c*, *Rassf2*, *Sarm1*) and immune

functions such as leukocyte activation (*Clec4a2*, *Dock8*, *Gpr183*, *Hdac5*, *Ifngr1*, *Notch1*), chemotaxis (*Ccr2*, *Cx3cr1*, *Cxcl14*, *Cx*cr3), and antigen presentation (*Fcgr3*, *H2-DMa*, *H2-DMb1*, *H2-DMb2*) were enriched in mRNAs with reduced abundance during infection by *L. donovani* promastigotes (**Fig 3A** lower panel, **Fig 3B** and **Table S2**).

Parasite stage-specific modulation of the host cell transcriptome during *L. donovani* infection

Anota2seq identified a subset of mRNAs (n=649) differentially regulated in the PRO- versus AMA-infected datasets (52.2% upregulated and 47.8% downregulated) (**Fig 4A** and **Table S1**). Comparison of this subset of transcripts with the AMA vs CTRL and PRO vs CTRL contrasts shown in **Fig. 1C** (**Table S1**) revealed a complex pattern of regulation with targets exhibiting a stage-exclusive (i.e. PRO only, AMA only), stage-enhanced (i.e. PRO enhanced, AMA enhanced) and stage-opposite (i.e. UP by PRO and DOWN by AMA, DOWN by PRO and UP by AMA) effects (**Figs 4B-C** and **Table S1**). In the upregulated PRO versus AMA dataset (n=339), *anota2seq* classified 70% of the transcripts as PRO only UP, 17% as AMA only DOWN, and 11% as PRO enhanced UP (i.e. UP by PRO and AMA but with a stronger effect in PRO) (**Fig 4B** and **Table S1**). In the downregulated PRO versus AMA dataset (n=310), *anota2seq* classified 69% of the transcripts as PRO only DOWN, 23% as AMA only UP, and 6% as PRO enhanced DOWN (i.e. DOWN by PRO and AMA but with a stronger effect in PRO) (**Fig 4B** and **Table S1**). In addition, 7 transcripts showed an enhanced effect by amastigotes (i.e. AMA enhanced, 3 UP and 4 DOWN) (**Fig 4B**, **Fig 4C**, right panel, and **Table S1**) whereas 7 transcripts were oppositely regulated between both stages, including 3 that were classified as PRO UP and AMA DOWN (*Acss2*, *Slc16a3*, *Slpi*), and 4 as PRO DOWN and AMA UP (*Bcr*, *Fcrls*, *Gcnt1*, *Id1*) (**Fig 4B**, **Fig 4C**, right panel, and **Table S1**).

Hierarchical clustering of transcripts identified as exclusively regulated upon amastigote infection (i.e. AMA only) revealed an enrichment of GO categories among upregulated transcripts encoding proteins associated with Immune signaling (*Cad*, *Ccl2*, *Wnk1*), DNA repair (*Mcm2*, *Nucks1*, *Pds5v*, *Rif1*, *Smc2*), and Transcription (*Etv1*, *Etv5*, *Myc*, *Rbl1*, *Sox4*), and Cell adhesion (*Icam1*, *Slfn1*) (**Fig 4C**, left panel, and **Table S2**) while downregulated targets exhibited an enrichment of GO categories associated with Immune response (*Ccl5*, *Cd14*, *H2-Aa*, *H2-Ab1*, *H2-Eb1*, *Il18bp*, *Irf7*, *Ly6c1*, *Ly6c2*, *Nfil3*) and Redox balance (*Folr1*, *Mgst1*, *Ppard*) (**Fig 4C**, left panel, and **Table S2**). The same type of analysis in the dataset of exclusively upregulated mRNAs upon promastigote infection (i.e. PRO only UP) identified GO categories related to Apoptosis regulation (i.e. *Cd274*, *Gclm*, *Optn*), Hydrogen peroxide metabolism (*Cat*, *Prdx1*, *Prdx6*, *Txnrd1*), Response to protozoan (*Cd40*, *Gbp2*, *Gbp3*, *Slc11a1*), and Response to type I IFN (*Ifit1*, *Ifit2*, *Igtp*, *Irgm1*, *Mnda*) (**Fig 4C**, middle panel, and **Table S2**). By contrast, transcripts exclusively downregulated by promastigotes (i.e. PRO only DOWN) were enriched in GO categories linked to Cell activation (*Ajuba*, *Gpr183*, *Hdac5*, *Tcf4*), Chemotaxis (*Arap3*, *Dab2*, *Dock1*, *Itga6*) and Cell signaling (*Btbd11*, *Nfatc2*, *Pak1*, *Pram1*) (**Fig 4C**, middle panel, and **Table S2**). The PRO enhanced UP subset showed an overrepresentation of apoptosis inhibitors (*Bcl2a1d*, *Gbe1*, *Gclc*, *Hmox1*, *Il1rn*, *Plk2*, *Serpinb9*) (**Fig 4C**, right panel, and **Table S2**) whereas no GO categories were enriched in the amastigote enhanced subset. Altogether, these results indicate that early infection by amastigotes or promastigotes of *L. donovani* elicits a selective and stage-specific transcriptional signature in macrophages involving mRNAs related to key cellular functions in disease progression.

Changes in host mRNA abundance upon *L. donovani* infection are associated with a network of upstream transcriptional regulators in macrophages

In order to identify potential upstream regulatory networks responsible for the changes in mRNA levels observed in BMDMs infected by the two life stages of *L. donovani*, we used Ingenuity® Pathway Analysis (IPA®). With an activation score $|Z| \geq 2.0$ and an FDR ≤ 0.01, IPA® identified subsets of transcripts with a regulatory trend predicted to be dependent on the activation or inhibition of different transcriptional modulators in BMDMs infected with *L. donovani* amastigotes or promastigotes (**Table S3**). Some upstream regulators were common between both parasite stages (MYC, KLF4, and SMAD3) albeit with variations in the number and/or identity of downstream targets in each type of infection (**Fig 5A** left panel and **S3 Table**). Others were predicted to be activated only by amastigotes (YY1, WDR5, and TP73) or promastigotes (NFE2L2, IRF7, IRF3, EPAS1, SPI1, NFATC2, ATF4, IFI16, CEBPB, CREB1, SP1, FOXO1, and FOS) (**Fig 5A** left panel and **Table S3**) while another group was predicted to be inhibited only upon infection with amastigotes (SOX6, RUNX3, and STAT1) or promastigotes (TRIM24 and FOXP3) (**Fig 5A** right panel and **Table S3**). Of note, Sirtuin 1 (SIRT1) was predicted to be activated in the amastigote-infected dataset whereas the opposite was found in the promastigote-infected dataset (**Fig 5A** and **Table S3**). As expected, transcriptional regulators predicted to be activated upon *L. donovani* infection showed high percentages of associated upregulated mRNAs (**Fig 5B**). These data hint at the involvement of a complex regulatory network affecting the abundance of functional subsets of mRNAs in BMDMs infected with *L. donovani* amastigotes or promastigotes.

Discussion

Accumulating evidence indicates that modulation of transcriptional profiles in infected macrophages is pathogen-specific[21]. Transcriptome-wide analyses of macrophages infected with *L. donovani* have been described at ≥ 12 h.p.i.[16-20,22], thereby omitting an earlier timeframe during which numerous molecular and cellular changes occurring within infected macrophages[8-10,23] could trigger, or be elicited by, selective reprogramming of the host transcriptome. Herein, using RNAseq, we describe rapid changes in the levels of mRNAs of primary murine macrophages infected with *L. donovani* amastigotes and promastigotes. Distinct transcriptional signatures were identified in macrophages infected with each parasite stage. A marked inhibition of mRNAs encoding proteins related to different immune functions was found in the amastigote-infected dataset whereas a combination of activating and inhibitory immune modulators was observed in promastigote-infected macrophages. Additionally, our *in sillico* analyses identified host mRNA signatures in the up- and downregulated datasets that appear to be under the control of parasite-stage driven networks of transcription factors. These observations indicate that amastigotes and promastigotes of *L. donovani* elicit a complex transcriptome-wide reprogramming in infected macrophages that includes both parasite stage-specific and commonly regulated mRNA subsets.

L. donovani amastigote-driven changes in macrophage gene expression have been documented at ≥ 24 h.p.i.[17,18,24]. Herein, we provide evidence that *L. donovani* amastigote infection leads to a vast remodelling of the macrophage transcriptome as early as 6 h.p.i. Among the downregulated targets, we found an enrichment in mRNAs encoding proteins related to several macrophage immune functions. IPA® predicted that some of these changes are dependent on the inhibition of

transcription factor STAT1. In this regard, Matte and Descoteaux previously reported that *L. donovani* amastigotes prevent STAT1 nuclear import and pro-inflammatory gene expression (i.e. *Nos2* and *Ifr1*) in BMDMs stimulated with IFNγ[12]. In addition, a transcriptomic study carried out in splenic macrophages revealed that these cells become insensitive to IFNγ during experimental VL despite a strong pro-inflammatory environment in the spleen[18]. Hence, it is plausible that early blockade of STAT1-dependent transcriptional programs in macrophages infected by *L. donovani* amastigotes has a negative effect in IFNγ-mediated microbicidal and immune host responses at later stages of the disease. Further investigation is required to shed light on this matter.

Infection of macrophages results in an oxidative burst response that involves the production of potent microbicidal effectors such as reactive oxygen and nitrogen species[25]. However, the antimicrobial oxidative stress response can also compromise macrophage DNA integrity and lead to the activation of apoptotic signals[26]. Our GO analyses showed an enrichment in mRNAs encoding DNA repair enzymes and inhibitors of apoptosis in the upregulated dataset of *L. donovani* amastigote-infected BMDMs at 6 h.p.i. Similarly, a proteome-based analysis of human macrophages infected with *L. donovani* identified DNA repair as an enriched ontology category reaching maximal values at 24 h.p.i.[27]. Moreover, among *L. donovani* promastigote- and amastigote-upregulated transcripts, we detected *Nbn*, which encodes a key member of the MRE11 DNA-damage-sensing complex[28]. Interestingly, *Nbn* is also induced in macrophages upon LPS-induced oxidative damage and serves as a modulator of macrophage homeostasis preventing attrition[29]. These reports along with our RNAseq data indicate *L. donovani* amastigotes elicit a cytoprotective transcriptional program to prevent oxidative-driven macrophage apoptosis at early stages of infection. Future studies are necessary to fully understand the molecular underpinnings

of parasite-driven activation of the host DNA repair machinery and its role in the establishment and progression of *L. donovani* infection within macrophages.

Leishmania parasites inhibit macrophage oxidative burst in order to survive[1]. Recently, Reverte *et al.* showed that expression of the transcription factor NRF2, a master regulator of the antioxidant response[30], is augmented during *Leishmania* spp. infection, including *L. donovani*[11]. Furthermore, upregulation of NRF2 activity contributed to promote parasite persistence during *L. guyanensis* infection by limiting inflammation[11]. In addition, NRF2-dependent increase in heme oxygenase 1 (HO-1) and ATF3 upon *L. donovani* infection was critical in dampening macrophage oxidative burst and proinflammatory cytokine expression as part of a parasite survival strategy[15]. Thus, our data showing an enrichment of transcripts associated with the activation of an NRF2-dependent antioxidant response (*Hmox1*, *Nqo1*, *Gsta3*, *Gstm1*) in promastigote-infected BMDMs suggest that targeting this regulatory node could be a therapeutic approach to combat VL.

In line with subversion of macrophage immune functions by *L. donovani* promastigotes[1], we identified a number of mRNAs encoding immune inhibitors in the upregulated promastigote-infected dataset, including *Cd274* (a.k.a. PDL1), *Socs1*, and *Cd200*. PDL1 and its receptor PD1 constitute an important inhibitory axis for T cell activity, and antibody therapy against PD1 has proven successful against numerous malignancies[31]. Notably, the PD1/PDL1 axis was recently identified to play an important role *in vivo* during VL and immunotherapy against PD1 was effective in hampering parasite burden and pathogenesis[22]. In addition, early induction of SOCS1, a known antagonist of the proinflammatory JAK1/STAT1 pathway[29,32], was identified as part of a

cellular program to prevent oxidative burst-mediated apoptosis in macrophages infected with *L. donovani*[33]. Similarly, a swift increase of CD200 in macrophages exposed to *L. amazonensis* or *L. donovani* infection was described as a strategy to favor parasite proliferation[34-36]. Interestingly, immune blockade of CD200 led to an increase in proinflammatory mediators and parasite elimination capacity of macrophages and T cells, showing its potential as a therapeutic target[36]. Taken together, these reports and our transcriptomic study highlight the early ability of *L. donovani* promastigotes to limit macrophage antimicrobial responses through the modulation of host mRNA abundance.

IPA® identified a transcriptional signature associated with type I interferon responses predicted to be activated via the transcription factors IRF3 and IRF7 in the promastigote-upregulated dataset. By contrast, downregulation of *Irf7* mRNA abundance was detected in the transcriptome of amastigote-infected BMDMs. IRF7-dependent parasite elimination was reported in macrophages of the splenic marginal zone during the acute phase of *L. donovani* amastigote infection *in vivo* (e.g. 5 to 48 h.p.i.) and by a cell line of stromal macrophages *in vitro.* Although the expression of IRF7 was not modulated in hepatic macrophages during VL, IRF7-defficient mice showed a decreased ability to control parasite burden in the liver[37]. These observations along with transcriptomic data and our *in sillico* analysis suggest that the ability of macrophages to elicit IRF7-dependent antimicrobial transcriptional programs upon *L. donovani* infection is tissue- and/or parasite-stage specific.

Our group recently described rapid remodeling of the translatome of macrophages infected by promastigotes and amastigotes of *L. donovani*[38]. Herein, we expanded our findings by analysing early changes in the abundance of host mRNAs during infection. Comparison of the transcriptome and the translatome of *L. donovani*-infected BMDMs at 6 h.p.i. indicates that in contrast to changes in translation efficiency[38], modulation of mRNA abundance is, at least in part, parasite stage-specific. Amastigote-driven changes included the upregulation of transcripts encoding for DNA repair modulators while inhibiting those encoding for antigen-presenting and macrophage activation factors. Alternatively, promastigote-infected macrophages showed the upregulation of immune inhibitors as well as an antioxidant transcriptional signature associated to NRF2 activity. However, enrichment of transcripts associated with IRF3 and IRF7 suggests that macrophages are able to activate antimicrobial pathways upon *L. donovani* promastigote infection. Interestingly, mRNAs encoding proteins associated with DNA damage-sensing or DNA repair, apoptosis inhibition and mRNA metabolism were upregulated via changes in abundance (**Figs 2 - 4**) and translation efficiency[38]. A similar dual effect was observed on a number of downregulated immune-related transcripts (e.g. antigen presentation, leukocyte activation, etc.)[38] (**Figs 2 - 4**). In all, previous studies, along with our current findings support the notion that early parasite-driven changes in macrophage gene expression programs are under the control of transcriptional and post-transcriptional regulatory mechanisms that tailor both protective and harmful host cell responses during *L. donovani* infection.

Materials and Methods

Reagents and Parasites

Culture media and supplements were purchased from Wisent, Gibco, and Sigma-Aldrich. *L. donovani* (LV9 strain) amastigotes were isolated from the spleen of infected female Golden Syrian hamsters (Harlan Laboratories) as previously described[12]. *L. donovani* (LV9 strain) promastigotes were differentiated from freshly isolated amastigotes and were cultured at 26°C in M199 medium supplemented with FBS (10%), hypoxanthine (100 μM), hemin (5 μM), biopterin (3 μM), biotin (1 μM), penicillin (100 U/mL), and streptomycin (100 μg/mL). Early passage stationary phase promastigotes were used for macrophage infections.

Ethics Statement

Housing and experiments were carried out under protocols approved by the Comité Institutionnel de Protection des Animaux (CIPA) of the INRS – Centre Armand-Frappier Santé Biotechnologie (CIPA 1308-04 and 1710-02). All methods were performed in accordance with relevant guidelines and regulations. These protocols respect procedures on good animal practice provided by the Canadian Council on animal care. The study is reported in accordance with ARRIVE guidelines.

Differentiation and infection of bone marrow-derived macrophages

Bone marrow-derived macrophages (BMDMs) were generated from precursor cells from murine bone marrow, as previously described[39]. Briefly, marrow was extracted from bones of the hind legs, red blood cells were lysed, and progenitor cells were resuspended in BMDM culture medium supplemented with 15% L929 fibroblast-conditioned culture medium (LCCM). Non-adherent cells were collected the following day and were cultured for 7 days in BMDM culture medium

supplemented with 30% LCCM with fresh medium replenishment at day 3 of incubation. BMDM cultures were inoculated with *L. donovani* promastigotes or amastigotes at a multiplicity of infection (MOI) of 10:1 for 6 h, as previously described[40]. Prior to infection, cells were serum-starved for 2 h.

Cytosolic mRNA extraction

Cytosolic lysates of infected and control BMDMs were prepared for RNA extraction as described[39]. RNA was extracted with QIAzol (Qiagen) and purified using RNeasy MinElute Cleanup Kit (Qiagen) according to specifications of the manufacturer. Purity and integrity of RNA was assessed using a Bioanalyzer 2100 with a Eukaryote Total RNA Nano chip (Agilent Technologies).

RNAseq and data processing

RNAseq libraries were generated using the Smart-seq2 method[41] and sequenced by using an Illumina HiSeq2500 instrument with a single-end 51-base sequencing setup from three independent biological replicates for uninfected and *L. donovani* promastigote-infected BMDMs, and five independent biological replicates for *L. donovani* amastigote-infected BMDMs. First, RNAseq reads mapping to the reference genome of the Nepalese BPK282A1 strain of *L. donovani* (txid: 981087) were removed (12.7% and 1.4% mappings on average for promastigotes and amastigotes, respectively). The filtered reads were then mapped to the mouse genome assembly GRCm38 (mm10) using HISAT2 with default settings[42]. Gene expression was quantified using the RPKMforgenes.py script[41] with -fulltranscript -readcount -onlycoding flags from which raw

per-gene RNAseq counts were obtained (version last modified 07.02.2014). Genes that had zero counts in all samples were discarded. Annotation of genes was obtained from RefSeq.

RNAseq data analysis using *anota2seq*

RNAseq counts were normalized within *anota2seq* using the default TMM-log2 method[43]. Significant changes in mRNA abundance were identified by *anota2seq*[43] using the default parameters with the following modifications: FDR ≤0.05; *apvEff* >$\log_2$(2.0). In *anota2seq*, the number of contrasts per analysis equals *n*-1 being *n* the number of conditions (i.e. CTR, *Ld* AMA, *Ld* PRO). In analysis one, infections were contrasted to the uninfected control (i.e. *Ld* PRO versus CTR and *Ld* AMA versus CTR); in analysis two, cells infected by different parasite stages were compared together and an additional contrast was included to complete the *anota2seq* parameters (i.e. *Ld* PRO vs *Ld* AMA and *Ld* PRO versus CTR). Identifiers for genes which cannot be distinguished based on their high sequence similarity (also reported by RPKMforgenes.py), were excluded from downstream analyses.

Gene ontology analyses

Gene ontology analyses were performed using the PANTHER™ tool[44] of the Gene Ontology Consortium (http://geneontology.org/) on the union of transcripts activated or inhibited in BMDMs infected by *L. donovani* amastigotes or promastigotes. Heatmaps of abundance of transcripts activated or inhibited in BMDMs infected by *L. donovani* amastigotes or promastigotes were generated using Morpheus.

(https://software.broadinstitute.org/morpheus/index.html, Broad Institute)

Ingenuity® Pathway Analysis

Enrichment of transcripts showing differential abundance in specific functional networks was determined using Ingenuity® Pathway Analysis (IPA®; Qiagen) by comparing *anota2seq*-regulated gene sets against the entire sequenced datasets[45]. Within the IPA® application, statistical significance was calculated using a right-tailed Fisher Exact test and p-values were adjusted for multiple hypothesis testing using the Benjamini-Hochberg method to arrive at a FDR.

Figure Captions

Figure 1. *L. donovani* infection leads to transcriptome-wide changes in macrophage mRNA abundance. (**A**) Strategy to identify cytosolic mRNAs that are regulated in *L. donovani* amastigote (AMA)- or promastigote (PRO)-infected BMDMs. RNAseq experiments were carried out in three to five biological replicates per condition. (**B**) Cytosolic mRNA datasets of BMDMs infected or not with *L. donovani* AMA or PRO were projected on the first two components of a principal component analysis. (**C**) Scatter plots of gene expression as RPKM (log_2) values for total cytosolic mRNA. Differentially regulated transcripts are indicated in red (Upregulated) or blue (downregulated). Unchanged mRNAs are shown in grey.

Figure 2. Selective changes in mRNA abundance predict amastigote-specific modulation of key biological processes in macrophages during *L. donovani* infection. (**A**) FDR values ($-log_{10}$) for selected GO term enriched categories of differentially up- or downregulated mRNAs upon *L. donovani* AMA infection. (**B**) Changes in mRNA abundance for selected genes in enriched GO terms. Analyses were carried out on data generated from at least three biological replicates.

Figure 3. Selective changes in mRNA abundance predict promastigote-specific modulation of key biological processes in macrophages during *L. donovani* infection. (**A**) FDR values ($-log_{10}$) for selected GO term enriched categories of differentially up- or downregulated mRNAs upon *L. donovani* PRO infection. (**B**) Changes in mRNA abundance for selected genes in enriched GO terms. Analyses were carried out on data generated from at least three biological replicates.

Figure 4. Parasite stage-driven changes in macrophage mRNA abundance during *L. donovani* infection. **(A)** Scatter plot of gene expression as RPKM (log_2) values for total mRNA between PRO and AMA datasets. Differentially regulated transcripts are indicated in red (Upregulated) or blue (downregulated). Unchanged mRNAs are shown in grey. (**B**) Category distribution of transcripts differentially regulated in macrophages upon *L. donovani* PRO versus AMA infection. (**C**) Heatmaps of selected transcripts differentially regulated only by amastigotes (left panel), promastigotes (center panel) or both (right panel). Manually curated ontology groups are shown for stage-specific regulated transcripts (left and middle panels). Analyses were carried out on data generated from at least three biological replicates.

Figure 5. Ingenuity® Pathway Analysis predicts parasite stage-specific modulation of transcriptional regulators in macrophages infected *L. donovani.* (**A**) Activation score (Z) of transcriptional regulators predicted to be involved in the changes of mRNA abundance in macrophages upon *L. donovani* AMA and PRO infection. *Common upstream regulators identified in PRO, AMA datasets by IPA®. (**B**) Percentage distribution of upregulated mRNAs associated with upstream transcriptional regulators predicted to be activated in macrophages upon *L. donovani* AMA and PRO infection. Total number of genes regulated by each transcription factor are shown in brackets. Analyses were carried out on data generated from at least three biological replicates.

406 **References**

407 1 Podinovskaia, M. & Descoteaux, A. Leishmania and the macrophage: a multifaceted
408 interaction. *Future microbiology* **10**, 111-129, doi:10.2217/fmb.14.103 (2015).

409 2 Khadem, F. & Uzonna, J. E. Immunity to visceral leishmaniasis: implications for
410 immunotherapy. *Future Microbiology* **9**, 901-915, doi:10.2217/fmb.14.43 (2014).

411 3 Burza, S., Croft, S. L. & Boelaert, M. Leishmaniasis. *Lancet* **392**, 951-970,
412 doi:10.1016/S0140-6736(18)31204-2 (2018).

413 4 Bhatt, D. M. *et al.* Transcript dynamics of proinflammatory genes revealed by sequence
414 analysis of subcellular RNA fractions. *Cell* **150**, 279-290, doi:10.1016/j.cell.2012.05.043
415 (2012).

416 5 Goldmann, O. *et al.* Transcriptome analysis of murine macrophages in response to
417 infection with Streptococcus pyogenes reveals an unusual activation program. *Infection*
418 *and immunity* **75**, 4148-4157, doi:10.1128/IAI.00181-07 (2007).

419 6 Li, Y. *et al.* Transcriptome Remodeling in Trypanosoma cruzi and Human Cells during
420 Intracellular Infection. *PLoS Pathogens* **12**, e1005511, doi:10.1371/journal.ppat.1005511
421 (2016).

422 7 Rabhi, S. *et al.* Lipid Droplet Formation, Their Localization and Dynamics during
423 Leishmania major Macrophage Infection. *PloS One* **11**, e0148640,
424 doi:10.1371/journal.pone.0148640 (2016).

425 8 Junghae, M. & Raynes, J. G. Activation of p38 mitogen-activated protein kinase attenuates
426 Leishmania donovani infection in macrophages. *Infection and immunity* **70**, 5026-5035,
427 doi:10.1128/IAI.70.9.5026-5035.2002 (2002).

9 Giri, J. *et al.* Leishmania donovani Exploits Myeloid Cell Leukemia 1 (MCL-1) Protein to Prevent Mitochondria-dependent Host Cell Apoptosis. *The Journal of biological chemistry* **291**, 3496-3507, doi:10.1074/jbc.M115.672873 (2016).

10 Matheoud, D. *et al.* Leishmania evades host immunity by inhibiting antigen cross-presentation through direct cleavage of the SNARE VAMP8. *Cell host & microbe* **14**, 15-25, doi:10.1016/j.chom.2013.06.003 (2013).

11 Reverte, M. *et al.* The antioxidant response favors Leishmania parasites survival, limits inflammation and reprograms the host cell metabolism. *PLoS pathogens* **17**, e1009422, doi:10.1371/journal.ppat.1009422 (2021).

12 Matte, C. & Descoteaux, A. Leishmania donovani amastigotes impair gamma interferon-induced STAT1alpha nuclear translocation by blocking the interaction between STAT1alpha and importin-alpha5. *Infection and immunity* **78**, 3736-3743, doi:10.1128/IAI.00046-10 (2010).

13 Phillips, R. *et al.* Innate killing of Leishmania donovani by macrophages of the splenic marginal zone requires IRF-7. *PLoS pathogens* **6**, e1000813, doi:10.1371/journal.ppat.1000813 (2010).

14 Saha, S. *et al.* Leishmania donovani Exploits Macrophage Heme Oxygenase-1 To Neutralize Oxidative Burst and TLR Signaling-Dependent Host Defense. *J Immunol* **202**, 827-840, doi:10.4049/jimmunol.1800958 (2019).

15 Saha, S., Roy, S., Dutta, A., Jana, K. & Ukil, A. Leishmania donovani Targets Host Transcription Factor NRF2 To Activate Antioxidant Enzyme HO-1 and Transcriptional Repressor ATF3 for Establishing Infection. *Infection and immunity* **89**, e0076420, doi:10.1128/IAI.00764-20 (2021).

16 Espitia, C. M. *et al.* Transcriptional profiling of the spleen in progressive visceral leishmaniasis reveals mixed expression of type 1 and type 2 cytokine-responsive genes. *BMC immunology* **15**, 38, doi:10.1186/s12865-014-0038-z (2014).

17 Gregory, D. J., Sladek, R., Olivier, M. & Matlashewski, G. Comparison of the effects of Leishmania major or Leishmania donovani infection on macrophage gene expression. *Infection and immunity* **76**, 1186-1192, doi:10.1128/IAI.01320-07 (2008).

18 Kong, F. *et al.* Transcriptional Profiling in Experimental Visceral Leishmaniasis Reveals a Broad Splenic Inflammatory Environment that Conditions Macrophages toward a Disease-Promoting Phenotype. *PLoS Pathogens* **13**, e1006165, doi:10.1371/journal.ppat.1006165 (2017).

19 Morimoto, A. *et al.* Hemophagocytosis induced by Leishmania donovani infection is beneficial to parasite survival within macrophages. *PLoS Neglected Tropical Diseases* **13**, e0007816, doi:10.1371/journal.pntd.0007816 (2019).

20 Shadab, M. *et al.* RNA-Seq Revealed Expression of Many Novel Genes Associated With Leishmania donovani Persistence and Clearance in the Host Macrophage. *Frontiers in Cellular and Infection Microbiology* **9**, 17, doi:10.3389/fcimb.2019.00017 (2019).

21 Chaussabel, D. *et al.* Unique gene expression profiles of human macrophages and dendritic cells to phylogenetically distinct parasites. *Blood* **102**, 672-681, doi:10.1182/blood-2002-10-3232 (2003).

22 Medina-Colorado, A. A. *et al.* Splenic CD4+ T Cells in Progressive Visceral Leishmaniasis Show a Mixed Effector-Regulatory Phenotype and Impair Macrophage Effector Function through Inhibitory Receptor Expression. *PloS One* **12**, e0169496, doi:10.1371/journal.pone.0169496 (2017).

23 Forestier, C. L., Machu, C., Loussert, C., Pescher, P. & Spath, G. F. Imaging host cell-Leishmania interaction dynamics implicates parasite motility, lysosome recruitment, and host cell wounding in the infection process. *Cell Host & Microbe* **9**, 319-330, doi:10.1016/j.chom.2011.03.011 (2011).

24 Smirlis, D. *et al.* SILAC-based quantitative proteomics reveals pleiotropic, phenotypic modulation in primary murine macrophages infected with the protozoan pathogen Leishmania donovani. *Journal of Proteomics* **213**, 103617, doi:10.1016/j.jprot.2019.103617 (2020).

25 Rendra, E. *et al.* Reactive oxygen species (ROS) in macrophage activation and function in diabetes. *Immunobiology* **224**, 242-253, doi:10.1016/j.imbio.2018.11.010 (2019).

26 Slupphaug, G., Kavli, B. & Krokan, H. E. The interacting pathways for prevention and repair of oxidative DNA damage. *Mutation Research* **531**, 231-251, doi:10.1016/j.mrfmmm.2003.06.002 (2003).

27 Singh, A. K. *et al.* Proteomic-based approach to gain insight into reprogramming of THP-1 cells exposed to Leishmania donovani over an early temporal window. *Infection and Immunity* **83**, 1853-1868, doi:10.1128/IAI.02833-14 (2015).

28 Pereira-Lopes, S. *et al.* NBS1 is required for macrophage homeostasis and functional activity in mice. *Blood* **126**, 2502-2510, doi:10.1182/blood-2015-04-637371 (2015).

29 Lopez-Sanz, L. *et al.* SOCS1-targeted therapy ameliorates renal and vascular oxidative stress in diabetes via STAT1 and PI3K inhibition. *Laboratory Investigation* **98**, 1276-1290, doi:10.1038/s41374-018-0043-6 (2018).

30 Vomund, S., Schafer, A., Parnham, M. J., Brune, B. & von Knethen, A. Nrf2, the Master Regulator of Anti-Oxidative Responses. *International Journal of Molecular Sciences* **18**, doi:10.3390/ijms18122772 (2017).

31 Sun, C., Mezzadra, R. & Schumacher, T. N. Regulation and Function of the PD-L1 Checkpoint. *Immunity* **48**, 434-452, doi:10.1016/j.immuni.2018.03.014 (2018).

32 Wei, H. *et al.* Suppression of interferon lambda signaling by SOCS-1 results in their excessive production during influenza virus infection. *PLoS Pathogens* **10**, e1003845, doi:10.1371/journal.ppat.1003845 (2014).

33 Srivastav, S. *et al.* Leishmania donovani prevents oxidative burst-mediated apoptosis of host macrophages through selective induction of suppressors of cytokine signaling (SOCS) proteins. *The Journal of Biological Chemistry* **289**, 1092-1105, doi:10.1074/jbc.M113.496323 (2014).

34 Cortez, M. *et al.* Leishmania promotes its own virulence by inducing expression of the host immune inhibitory ligand CD200. *Cell Host & Microbe* **9**, 463-471, doi:10.1016/j.chom.2011.04.014 (2011).

35 Sauter, I. P. *et al.* TLR9/MyD88/TRIF signaling activates host immune inhibitory CD200 in Leishmania infection. *JCI insight* **4**, doi:10.1172/jci.insight.126207 (2019).

36 Rawat, A. K. *et al.* The CD200-CD200R cross-talk helps Leishmania donovani to down regulate macrophage and CD4(+)CD44(+) T cells effector functions in an NFkappaB independent manner. *International Journal of Biological Macromolecules* **151**, 394-401, doi:10.1016/j.ijbiomac.2020.02.189 (2020).

37 Beattie, L. *et al.* Interferon regulatory factor 7 contributes to the control of Leishmania donovani in the mouse liver. *Infection and Immunity* **79**, 1057-1066, doi:10.1128/IAI.00633-10 (2011).

38 Chaparro, V. *et al.* Translational profiling of macrophages infected with Leishmania donovani identifies mTOR- and eIF4A-sensitive immune-related transcripts. *PLoS Pathogens* **16**, e1008291, doi:10.1371/journal.ppat.1008291 (2020).

39 Leroux, L. P. *et al.* The Protozoan Parasite Toxoplasma gondii Selectively Reprograms the Host Cell Translatome. *Infection and Immunity* **86**, doi:10.1128/IAI.00244-18 (2018).

40 Atayde, V. D. *et al.* Exploitation of the Leishmania exosomal pathway by Leishmania RNA virus 1. *Nature Microbiology* **4**, 714-723, doi:10.1038/s41564-018-0352-y (2019).

41 Ramskold, D., Wang, E. T., Burge, C. B. & Sandberg, R. An abundance of ubiquitously expressed genes revealed by tissue transcriptome sequence data. *PLoS Computational Biology* **5**, e1000598, doi:10.1371/journal.pcbi.1000598 (2009).

42 Kim, D., Langmead, B. & Salzberg, S. L. HISAT: a fast spliced aligner with low memory requirements. *Nature Methods* **12**, 357-360, doi:10.1038/nmeth.3317 (2015).

43 Oertlin, C. *et al.* Generally applicable transcriptome-wide analysis of translation using anota2seq. *Nucleic Acids Research* **47**, e70, doi:10.1093/nar/gkz223 (2019).

44 Mi, H. *et al.* PANTHER version 11: expanded annotation data from Gene Ontology and Reactome pathways, and data analysis tool enhancements. *Nucleic Acids Research* **45**, D183-D189, doi:10.1093/nar/gkw1138 (2017).

45 Kramer, A., Green, J., Pollard, J., Jr. & Tugendreich, S. Causal analysis approaches in Ingenuity Pathway Analysis. *Bioinformatics* **30**, 523-530, doi:10.1093/bioinformatics/btt703 (2014).

Figures

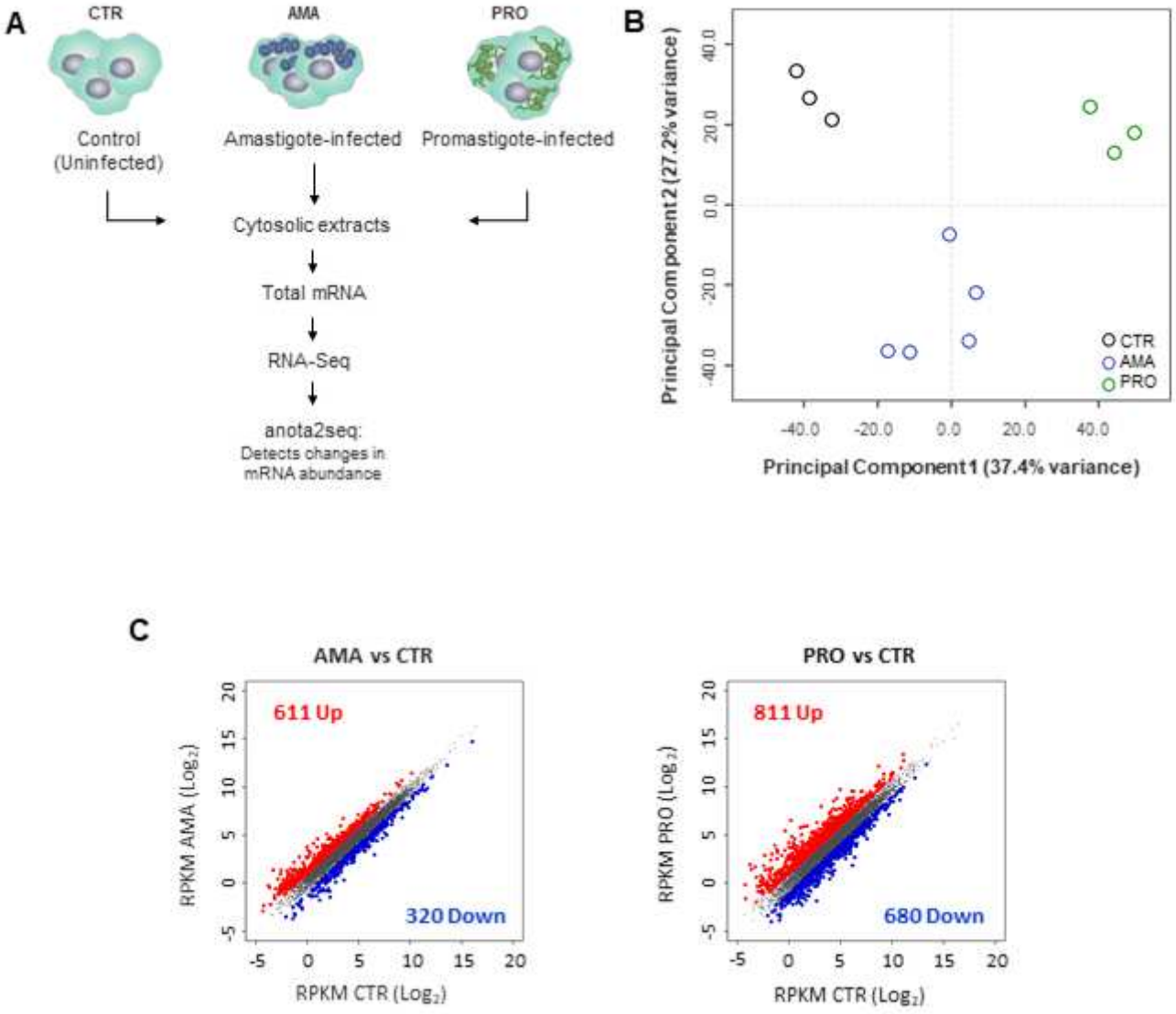

Figure 1

L. donovani infection leads to transcriptome-wide changes in macrophage mRNA abundance. (A) Strategy to identify cytosolic mRNAsthat are regulated in L. donovani amastigote (AMA)- or promastigote (PRO)-infected BMDMs. RNAseq experiments were carried out in three to five biological replicates per condition. (B) Cytosolic mRNA datasets of BMDMs infected or not with L. donovani AMA or PRO were projected on the first two components of a principal component analysis. (C) Scatter plots of gene expression as RPKM (log2) values for total cytosolic mRNA. Differentially regulated transcripts are indicated in red (Upregulated) or blue (downregulated). Unchanged mRNAs are shown in grey.

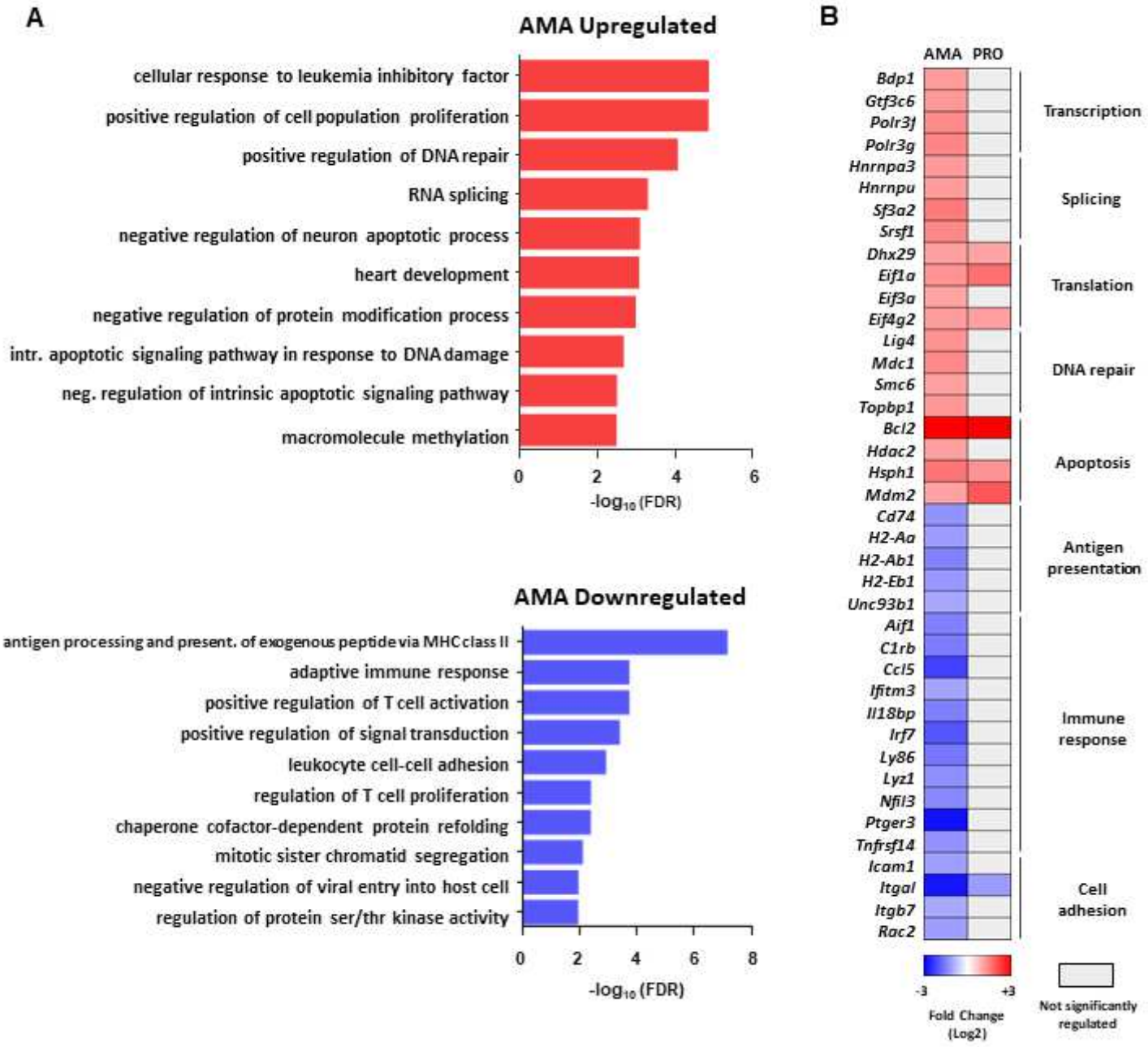

Figure 2

Selective changes in mRNA abundance predict amastigote-specific modulation of key biological processes in macrophages during L. donovani infection. (A) FDR values (-log10) for selected GO term enriched categories of differentially up- or downregulated mRNAs upon L. donovani AMA infection. (B) Changes in mRNA abundance for selected genes in enriched GO terms. Analyses were carried out on data generated from at least three biological replicates.

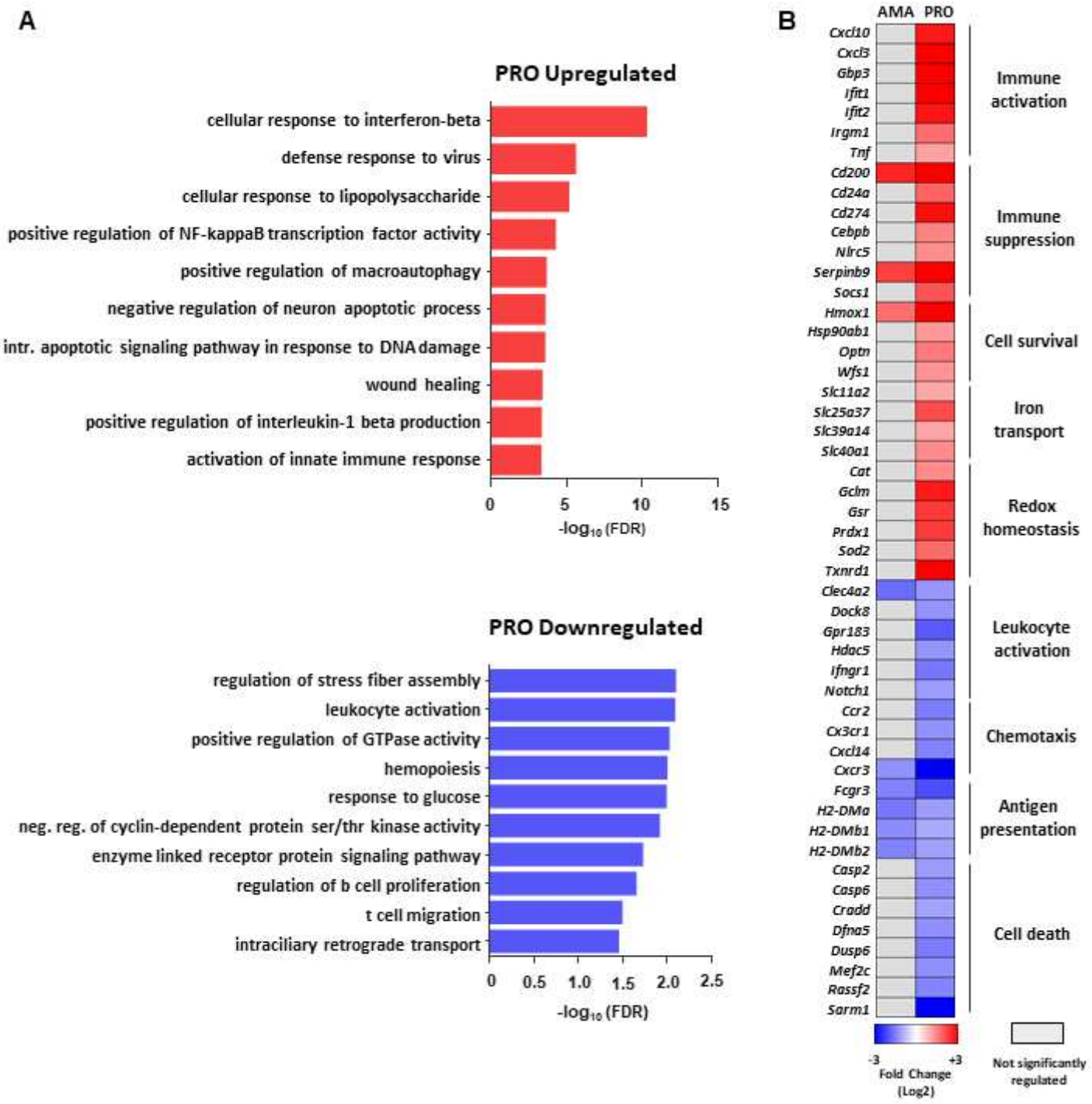

Figure 3

Selective changes in mRNA abundance predict promastigote-specific modulation of key biological processes in macrophages during L. donovani infection. (A) FDR values (- log10) for selected GO term enriched categories of differentially up- or downregulated mRNAs upon L. donovani PRO infection. (B) Changes in mRNA abundance for selected genes in enriched GO terms. Analyses were carried out on data generated from at least three biological replicates.

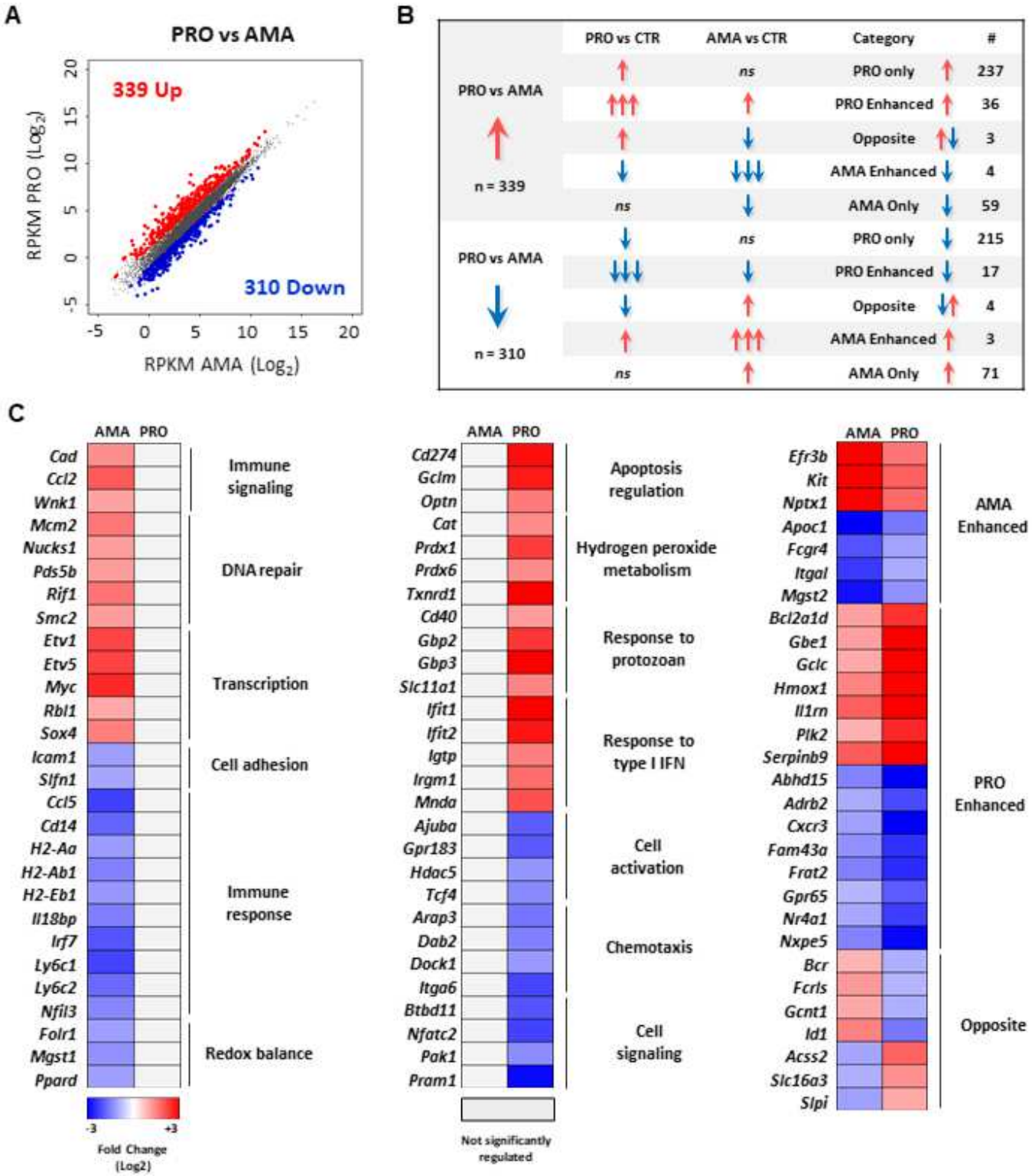

Figure 4

Parasite stage-driven changes in macrophage mRNA abundance during L. donovani infection. (A) Scatter plot of gene expression as RPKM (log2) values for total mRNA between PRO and AMA datasets. Differentially regulated transcripts are indicated in red (Upregulated) or blue (downregulated). Unchanged mRNAs are shown in grey. (B) Category distribution of transcripts differentially regulated in macrophages upon L. donovani PRO versus AMA infection. (C) Heatmaps of selected transcripts differentially regulated

only by amastigotes (left panel), promastigotes (center panel) or both (right panel). Manually curated ontology groups are shown for stage-specific regulated transcripts (left and middle panels). Analyses were carried out on data generated from at least three biological replicates.

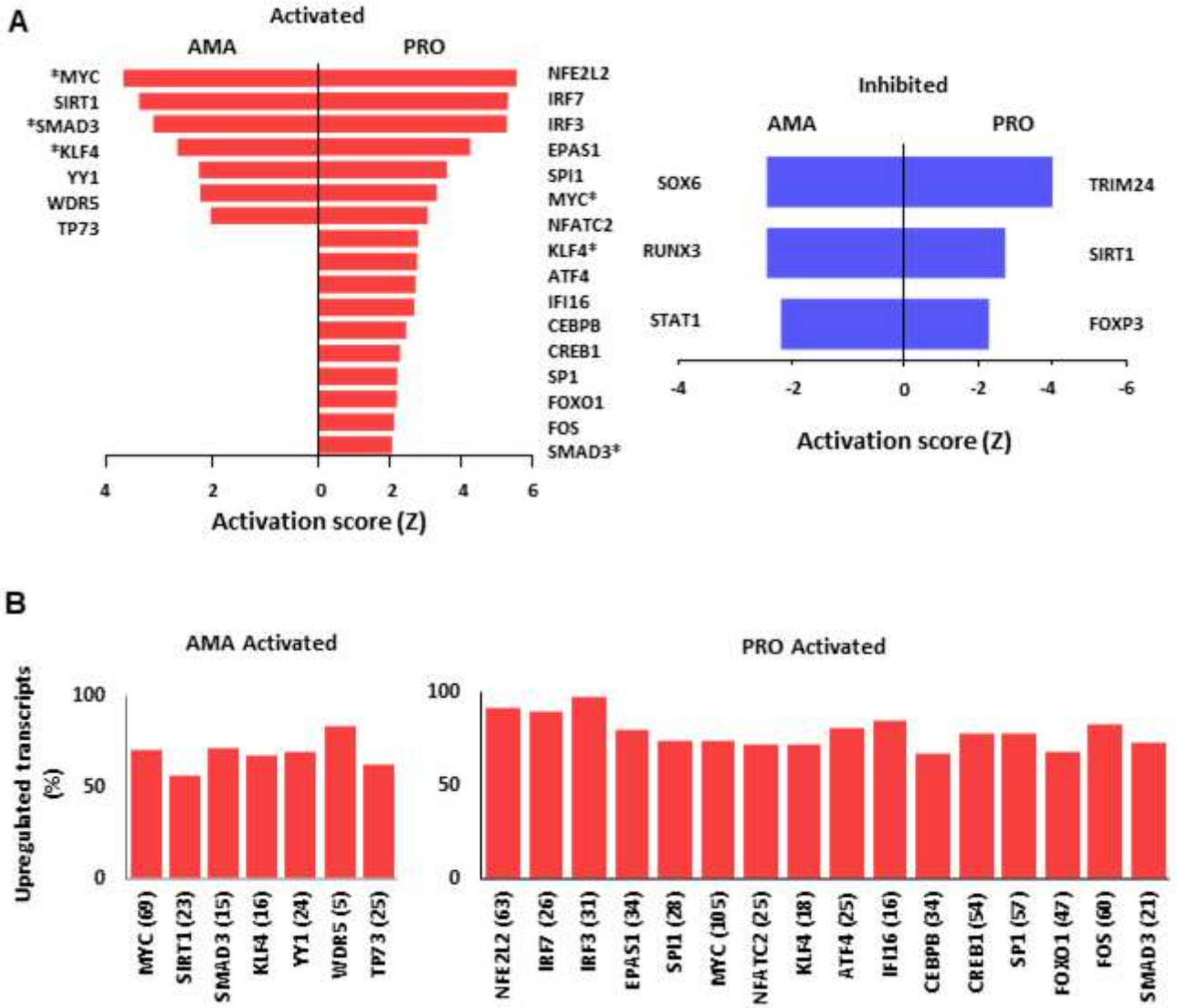

Figure 5

Ingenuity® Pathway Analysis predicts parasite stage-specific modulation of transcriptional regulators in macrophages infected L. donovani. (A) Activation score (Z) of transcriptional regulators predicted to be involved in the changes of mRNA abundance in macrophages upon L. donovani AMA and PRO infection. *Common upstream regulators identified in PRO, AMA datasets by IPA®. (B) Percentage distribution of upregulated mRNAs associated with upstream transcriptional regulators predicted to be activated in macrophages upon L. donovani AMA and PRO infection. Total number of genes regulated by each transcription factor are shown in brackets. Analyses were carried out on data generated from at least three biological replicates.

Supplementary Files

This is a list of supplementary files associated with this preprint. Click to download.

- ChaparroetalTableS1.xlsx
- ChaparroetalTableS2.xlsx
- ChaparroetalTableS3.xlsx